

Rethinking Domain Generalization: Discriminability and Generalizability

Shaocong Long^{*}, Qianyu Zhou^{*}, Chenhao Ying[†], Lizhuang Ma, Yuan Luo[†]

Abstract—Domain generalization (DG) endeavours to develop robust models that possess strong generalizability while preserving excellent discriminability. Nonetheless, pivotal DG techniques tend to improve the feature generalizability by learning domain-invariant representations, inadvertently overlooking the feature discriminability. On the one hand, the simultaneous attainment of generalizability and discriminability of features presents a complex challenge, often entailing inherent contradictions. This challenge becomes particularly pronounced when domain-invariant features manifest reduced discriminability owing to the inclusion of unstable factors, *i.e.*, spurious correlations. On the other hand, prevailing domain-invariant methods can be categorized as category-level alignment, susceptible to discarding indispensable features possessing substantial generalizability and narrowing intra-class variations. To surmount these obstacles, we rethink DG from a new perspective that concurrently imbues features with formidable discriminability and robust generalizability, and present a novel framework, namely, Discriminative Microscopic Distribution Alignment (DMDA). DMDA incorporates two core components: Selective Channel Pruning (SCP) and Micro-level Distribution Alignment (MDA). Concretely, SCP attempts to curtail redundancy within neural networks, prioritizing stable attributes conducive to accurate classification. This approach alleviates the adverse effect of spurious domain-invariance and amplifies the feature discriminability. Besides, MDA accentuates micro-level alignment within each class, going beyond mere category-level alignment. This strategy accommodates sufficient generalizable features and facilitates within-class variations. Extensive experiments on four benchmark datasets corroborate that DMDA achieves comparable results to state-of-the-art methods in DG, underscoring the efficacy of our method. The source code will be available at <https://github.com/longshaocong/DMDA>.

Index Terms—Domain generalization, representation learning, discriminability, generalizability, transfer learning.

I. INTRODUCTION

COMPUTER vision has achieved remarkable success in image classification [1]–[5], image segmentation [6]–[8], and object detection [9]–[13]. Nonetheless, real-world data frequently experiences distribution shifts [14]–[20] across distinct scenarios, significantly impairing the performance of learned models [21], [22]. Such distribution shifts may arise from multiple factors, such as alterations in background [23], changes in visual angles [24], and camera’s field of views [25],

S. Long, Q. Zhou, C. Ying, L. Ma, Y. Luo are with the Department of Computer Science and Engineering, Shanghai Jiao Tong University, Shanghai 200240, China (email: {longshaocong, zhouqianyu, yingchenhao, yuanluo}@sjtu.edu.cn and ma-lz@cs.sjtu.edu.cn). C. Ying and Y. Luo are also with Shanghai Jiao Tong University (Wuxi) Blockchain Advanced Research Center. This work was supported in part by National Key R&D Program of China under Grant 2022YFA1005000.

^{*}Equal contributions, [†]Corresponding authors.

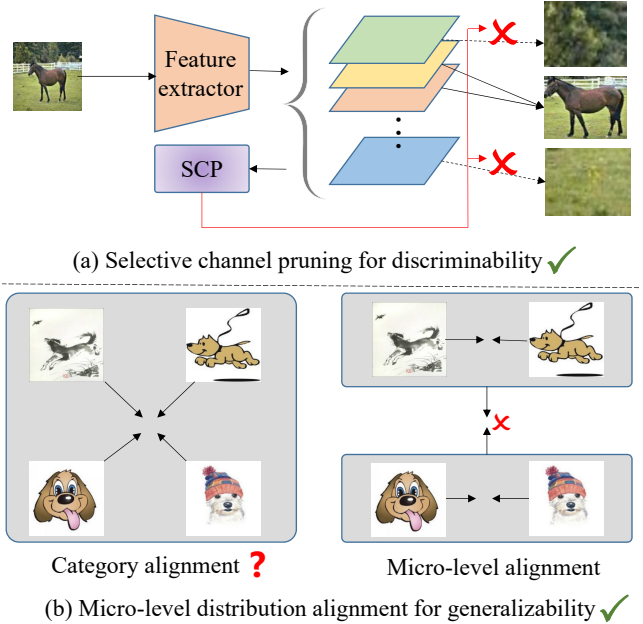


Fig. 1. Almost all DG methods tend to improve the feature generalizability by learning domain-invariant representations, and inadvertently overlook the feature discriminability, leading to spurious domain invariance. (a) To boost the feature discriminability, we propose Selective Channel Pruning (SCP) to filter out unstable factors, *i.e.*, spurious correlations, thereby mitigating the adverse effects of such correlations. (b) Besides, we introduce Micro-level Distribution Alignment (MDA) to prevent the risk of discarding indispensable generalizable features in previous category-level distribution alignment. MDA could accommodate sufficient generalizable features while simultaneously enhancing within-class variations, thereby promoting feature generalizability.

and *etc.*. The degrading performance originates from spurious correlations captured by the model trained in limited training environments. Taking the image classification [23] as an instance, the hypothesis model suffers from recognizing cows on the beach due to the background shift from grassland to beach. In such case, the model may rely solely on the background instead of focusing on the presence of animals for classification. As such, the model’s ability to generalize to out-of-sample scenarios is compromised.

Numerous efforts have been dedicated to enhancing models’ generalization capacities [24], [26]–[29], with the purpose of capturing genuine correlations from biased data. Unsupervised domain adaptation (UDA) [18], [19], [30]–[36] stands as an effective technique to mitigate distribution shifts. Nonetheless, these models require access to the target data during the training phase and thereby necessitate adaption when new scenarios occur, which is time-consuming and impractical in real-world scenarios. A more challenging avenue to address

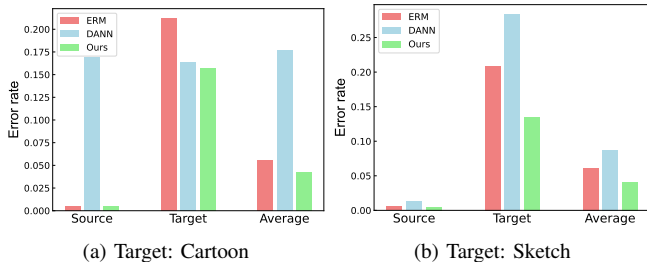


Fig. 2. Comparisons of classification error rates on the feature representations. The error rate measures the discriminability of acquired features.

distribution shift is domain generalization (DG) [37]–[42], which has no access to the target data during training and exclusively leverages information from source domains.

Current approaches in DG tend to improve the feature generalizability via learning domain-invariant representations [30], [39], [43]–[45] while overlooking and compromising the feature discriminability. It is noteworthy that there is an inconsistency in simultaneously improving the generalizability and discriminability of features. Fig. 2 measures the feature discriminability by measuring the classification error rate with the acquired features. As observed, the error rate on the representation of DANN [30] exceeds that of ERM in most scenarios, indicating the reduced feature discriminability by DANN. Consequently, it is significant to mitigate the mutual influence between generalizability and discriminability. However, it is non-trivial to design an effective DG mechanism to trade off the generalizability and discriminability that is applicable in various scenarios. On the one hand, excessive emphasis on feature discriminability compromises the generalizability. On the other hand, excessive focus on generalizability poses the peril of generating features deficient in discrimination. We argue that the crux lies in the unstable factors, *i.e.*, spurious correlations. When acquired features lack stable relevance to classification, pursuing domain-invariance on such features becomes futile and may even intensify source risks. Hence, it is crucial to enforce domain-invariance upon stable factors, which can mitigate the adverse effect of unstable factors on the consistency between generalizability and discriminability.

In addition to addressing the challenges posed by unstable factors, it is essential to acknowledge that achieving domain-invariant learning can be an intricate endeavor. Conventional domain-invariant learning is characterized as category alignment, wherein the predominant approach seeks to mitigate disparities amongst prototypes or semantics of samples within each category across domains [38], [39], [43], [46]–[48]. However, such category alignment inherently is a coarse-grained alignment strategy and may confront difficulties in learning sufficient generalizable features. This is chiefly attributed to the relative substantial divergence in attributes for samples within the same category, rendering the coarse-grained alignment for a specific category across domains potentially liable to discard indispensable features possessing substantial generalizability. As illustrated in Fig. 1(b), there is a significant disparity between running dogs and dogs depicted with only their heads. Attempting to align them forcibly could result in the loss of distinctive features associated with the

dog’s body and legs. Therefore, it is significant to relax the stringent constraints of category-level domain-invariance. In doing so, we focus on aligning the distributions of samples within a category that have similar semantics, without mandating alignment for samples with distant semantics within the same category. This way also serves to enrich the within-class variations, a known catalyst for enhancing generalization performance [49], [50].

To surmount the aforementioned limitations, we rethink DG through the lens of feature discriminability and generalizability. In this work, we present a novel framework, named Discriminative Microscopic Distribution Alignment (DMDA). This framework comprises two innovative modules: Selective Channel Pruning (SCP) and Micro-level Distribution Alignment (MDA), which collaborate to elevate the feature discriminability and generalizability. Fig. 1 illustrates the two key modules in our proposed approach. Specifically, SCP filters out the unstable channels in features and curtails redundancy within neural networks to enhance feature discriminability. Besides, MDA performs distribution alignment at the micro level rather than the category level to promote feature generalizability. Compared with existing domain-invariant methods in DG, our approach offers dual advantages: Firstly, our model focuses on stable correlations, aiming to heighten the feature discriminability. Secondly, our strategy guarantees micro-level invariance, facilitating the acquisition of sufficient generalizable features and accommodating within-class variations. Consequently, our proposed approach not only augments feature generalizability across domains but also enhances category-level discriminability, resulting in superior generalization capacities of models. In summary, our main contributions include:

- We introduce a novel perspective for DG with the dual objectives of enhancing feature generalizability while concurrently improving discriminability.
- We present an innovative approach named DMDA for DG, comprising two key modules: SCP and MDA. Concretely, SCP mitigates the detrimental effect of spurious correlations, thereby endowing the acquired features with heightened discriminability. While MDA pursues domain invariance at the micro level, rather than the category level, boosting feature generalizability.
- Extensive experiments on four benchmark datasets corroborate the efficacy and superiority of the proposed approach, where it achieves competitive performance compared to state-of-the-art methods in DG.

II. RELATED WORK

Techniques from diverse perspectives have been proposed to improve models’ generalization capacity in DG.

One notable research avenue is domain-invariant learning [37], [43], [51], [52]. The objective is to cultivate common features across domains that possess the potential to generalize effectively to novel scenarios. Denote the input, acquired features, and output as X , Φ , and Y , respectively. A foundational approach, proposed by Ganin *et al.* [30] as Domain Adversarial Training of Neural Networks (DANN), seeks to

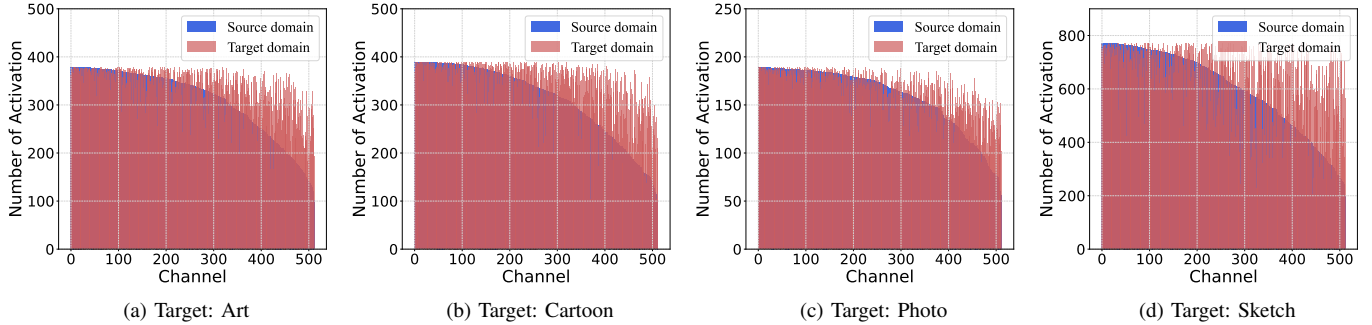


Fig. 3. The channel activation frequency in the penultimate layer of ResNet-18 trained via ERM, with ‘Art’, ‘Cartoon’, ‘Photo’, and ‘Sketch’ as the target domain, respectively. Channels are arranged in descending order based on the activation frequency in source domains. Channels experiencing infrequent activation in source domains but displaying frequent activation in target domain can be characterized as unstable factors demonstrating spurious correlations.

acquire domain-invariant features through adversarial learning, under the assumption that the conditional distribution $P(Y|X)$ remains invariant. However, this assumption may not hold in practical settings, leading to DANN’s limitations. To address this limitation, Li *et al.* [53] proposed a conditional adversarial network to satisfy the invariant distribution $P(\Phi|Y)$, considering the causal direction $Y \rightarrow X$ and assuming class-balance in the target data. Alternatively, Zhao *et al.* [39] proposed minimizing the divergence between conditional distributions across domains, ensuring the invariant conditional distribution $P(Y|\Phi)$. Additionally, self-supervised learning [54]–[58] has made notable contributions to improve the expressive power of features. SelfReg [59] and PCL [48], for instance, took advantage of contrastive learning to encourage representations to be close for samples within the same class and distant from samples in other classes. Besides, a heightened awareness has emerged regarding the robustness of feature maps [60], [61]. These methods are directed towards suppressing domain-sensitive information from a feature map perspective.

Another intuitive approach is to expand the source domains through data augmentation [17], [62]–[64] or data generation [65], thus indirectly decreasing the distribution gap between source and target domains. For instance, Zhou *et al.* [66] proposed a transformation for data augmentation using adversarial training. Rahman *et al.* [67] employed ComBoGAN [68] to generate new data with a small distribution discrepancy to the original data.

Ensembling techniques [59], [69], [70] have been introduced to seek flatter minima, which has been proven an effective strategy for enhancing generalization performance. SelfReg [59] and SWAD [69] utilized Stochastic Weights Averaging to find the flatter minima, consequently reducing the domain generalization gap in the target domain.

Different from prevailing approaches primarily focused on enhancing the generalizability of acquired features in DG, this study endeavors to concurrently elevate both feature discriminability and generalizability.

III. METHODOLOGY

A. Preliminaries

Let \mathcal{X} and \mathcal{Y} denote the input space and output space, respectively. In DG, there are M source (seen) domains $S_{source} = \{S^i | i = 1, 2, \dots, M\}$ where $S^i = \{(x_j^i, y_j^i) | j =$

$1, 2, \dots, n_i\} \sim P_i^S(X, Y)$. Here, n_i is the number of samples in domain S^i , and $P_i^S(X, Y)$ is the joint distribution of the covariates together with labels in domain S^i , which is different from that of other domains: $P_i^S(X, Y) \neq P_j^S(X, Y), i \neq j$. We assign $U_{source} = \{U^i | i = 1, 2, \dots, M\}$ as the domain-dependent variables (style, background, *etc.*), which vary across domains: $U^i \neq U^j, i \neq j$. Given the source domains, the goal of DG is to learn a robust model $h = g \circ f$, where $f : X \rightarrow \Phi$ is the representation function and $g : \Phi \rightarrow Y$ is the label predictive function. This model is expected to generalize well to the N target (unseen) domains $T_{target} = \{T^i | i = 1, 2, \dots, N\}$ where $T^i = \{(x_j^i, y_j^i) | j = 1, 2, \dots, n_i\} \sim P_i^T(X, Y)$. The distributions in source domains and target domains are different: $P^S(X, Y) \neq P^T(X, Y)$. Besides, the target domains cannot be accessed during the training phase.

In this section, we elucidate our strategy for overcoming the inherent constraints of domain-invariant methods in DG, endowing the acquired features with both robust generalizability and formidable discriminability. Fig. 4 illustrates the overall architecture of our proposed Discriminative Microscopic Distribution Alignment (DMDA), encompassing two key modules, namely Selective Channel Pruning (SCP) and Micro-level Distribution Alignment (MDA). SCP serves to ameliorate the impact of unstable factors on the features discriminability, while MDA augments features’ generalizability through micro-level distribution alignment. Specifically, the features acquired through the feature extractor traverse through SCP to derive channel-wise masks, which are subsequently employed for feature pruning. Subsequently, MDA aligns micro-level distributions of the pruned features, guided by the underlying semantics of the pruned features.

B. Selective Channel Pruning

Prevalent DG methods strive to enhance feature generalizability by acquiring domain-invariant representations, often inadvertently sidelining discriminability. Nevertheless, the relentless pursuit of domain invariance can yield features with subpar discriminability, posing a formidable challenge for the classification. As illustrated in Fig. 2, the drive for domain invariance by DANN [30] can lead to diminished feature discriminability. This dilemma arises from the conflict between the concurrent enhancement of both generalizability and discriminability. We posit that this may result from unstable fac-

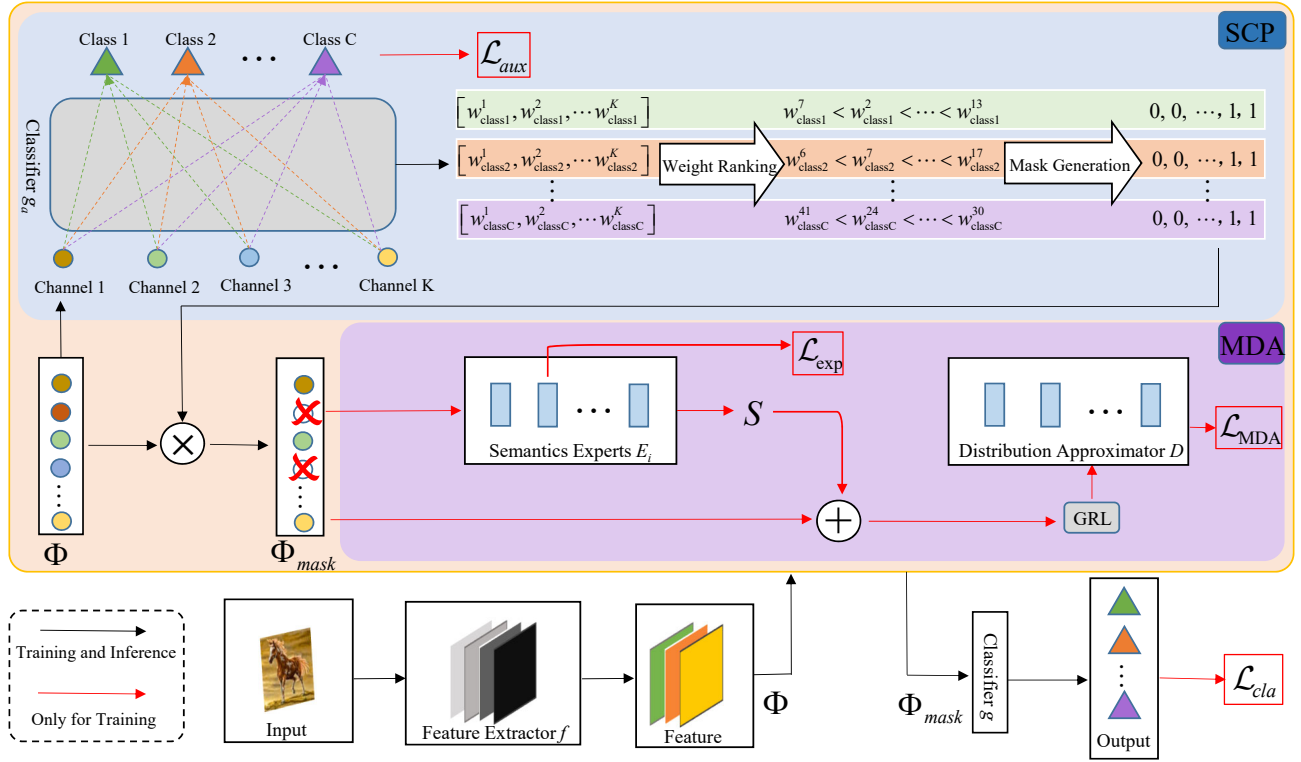


Fig. 4. **Framework of our proposed Discriminative Microscopic Distribution Alignment (DMDA).** The features generated by the feature extractor are initially transmitted to the Selective Channel Pruning (SCP) module to create channel-wise masks for the purpose of eliminating unstable channels. Following this, the features undergo pruning based on the channel-wise masks. Subsequently, Micro-level Distribution Alignment (MDA) is employed to execute micro-level distribution alignment rooted in the latent semantics of the pruned features, which are generated by additional semantics experts.

tors, *i.e.*, spurious correlations, which induce spurious domain invariance while concurrently impeding discriminability.

To succeed in a classification task, it is imperative that the acquired features encapsulate only the stable factors carrying essential information while discarding spurious correlations. The current solution typically seeks to minimize the empirical risk across source domains:

$$\mathcal{L}_{cla} = \sum_{i=1}^M \sum_{x,y} P_i^S(x,y) \ell(h(x), y), \quad (1)$$

where ℓ denotes the cross-entropy loss. However, the straightforward approach cannot guarantee the stability of every dimension in the acquired features. This implies that certain dimensions may convey spurious correlations for classification and consequently offer limited utility for generalization.

Based on the above insight, we explore the stability of different channels to enhance generalization performance. When considering a specific class, channels carrying genuine information tend to manifest more generalized patterns and should be activated with greater frequency. Conversely, channels capturing spurious correlations should experience less frequent activation due to the distribution shift across source domains. To gain a comprehensive understanding of this phenomenon, we visualize the channel activation frequency within source domains and target domains in Fig. 3, respectively. A channel is considered activated if its activation value exceeds a threshold (1% of the highest activation value across all channels in our case.). In this visualization, we take the class

‘dog’ as an instance, and analyze the activation frequency of each channel for samples in source domains and target domains, respectively. We arrange the channels in descending order based on the activation frequency of samples in source domains. It is noteworthy that we have adjusted the number of samples in the target domain to ensure a fair comparison. As depicted in Fig. 3, samples from source domains and target domains exhibit different activation patterns. Samples in target domains frequently activate channels that receive less frequent activation from samples in source domains. This trend persists across all classes. The channels that are less frequently activated in source domains and display inconsistencies in activation frequency between the source and target domains can be identified as unstable channels, containing spurious correlations that are detrimental to generalization.

The above observation motivates us to propose an unstable factor removal strategy, Selective Channel Pruning (SCP), to mitigate the adverse effects of unstable factors on generalization capacities. Denote the output of l -th activation layer of the model h as $\Phi^l \in \mathbb{R}^{H \times W \times K}$, where H , W , and K represent the height, width, and number of channels, respectively. In the SCP module, we begin by applying the Global Average Pooling (GAP) operation on the raw feature map, resulting in the channel-wise activation $\hat{\Phi}^l \in \mathbb{R}^K$. Mathematically, the activation of the k -th channel can be defined as:

$$\hat{\Phi}^l = \frac{1}{H \times W} \sum_{i=1}^H \sum_{j=1}^W \Phi_k^l(i, j). \quad (2)$$

We then input the channel-wise activation $\hat{\Phi}^l$ into an auxiliary classifier g_a , which can be optimized by minimizing the risk:

$$\mathcal{L}_{aux} = \sum_{i=1}^M \sum_{x,y} P_i^S(x,y) \ell(g_a(\hat{\Phi}^l), y). \quad (3)$$

This classifier consists of only one fully connected (FC) layer to perform classification. Considering a classification task with C classes, we denote the parameters of this auxiliary classifier as $W_l = [W_1^l, W_2^l, \dots, W_C^l] \in \mathbb{R}^{K \times C}$, which assesses the significance of each channel to a specific class. To mitigate the adverse effects of unstable channels, we introduce a pruning strategy that takes into account the channels' significance in the classification. More specifically, the pruning strategy for i -th channel of class c can be mathematically formulated as:

$$M_{c,i}^l = \begin{cases} 0, & W_{c,i}^l \leq Q_q(W_c^l) \\ 1, & W_{c,i}^l > Q_q(W_c^l) \end{cases}, \quad (4)$$

where Q_q represents q -th percentile for W_c^l , serving as the criterion for identifying whether channels are selected as stable channels. Subsequently, we employ these masks to reconstruct the original feature maps in a channel-wise manner. During the training stage, we adopt the ground-truth label y as the reference to determine channel importance and generate channel masks. However, during the testing stage when access to the ground-truth label y is unavailable, we employ the index (denoted as \bar{y}) associated with the maximum value in the predicted labels to determine the channel importance and the channel mask selection. The resultant masked channels can be represented as:

$$\Phi_{mask}^l = \begin{cases} \Phi^l \otimes M_y^l, & \text{training phase} \\ \Phi^l \otimes M_{\bar{y}}^l, & \text{test phase} \end{cases}, \quad (5)$$

where \otimes denotes channel-wise multiplication. The pruned feature maps rather than the original feature maps will be propagated into the subsequent layer.

C. Micro-level Distribution Alignment

Methods based on domain-invariant representation learning have garnered significant attention in DG. Given the assumption that the conditional distribution $P(Y|X)$ stays invariant, Ganin *et al.* [30] proposed domain adversarial training of neural networks (DANN) for domain adaptation, which aims to cultivate domain-invariant features Φ through adversarial learning. To address the limitation posed by assuming invariant conditional distributions, Li *et al.* [53] presented a conditional adversarial network to satisfy the invariant distribution $P(\Phi|Y)$, while considering the causal direction $Y \rightarrow X$ and assuming class-balance in the target data. As an alternative and effective strategy, Zhao *et al.* [39] proposed minimizing the divergence between conditional distributions across domains to ensure the invariant conditional distribution $P(Y|\Phi)$.

While these domain-invariant methods have made strides by aligning the marginal and conditional distributions, they overlook a critical aspect: As category alignment, these methods inherently are coarse-grained alignment strategies. The coarse-grained alignment is a rather strict constraint and may result

in information loss within categories. Consequently, category alignment methods encounter challenges in acquiring an adequate pool of generalizable features. This challenge primarily arises due to significant variations in attributes among samples within the same category. Such variations make coarse-grained alignment strategies for specific categories across domains prone to the inadvertent exclusion of essential features that hold significant generalizability.

To mitigate the adverse effects linked to category alignment in DG, we introduce Micro-level Distribution Alignment (MDA). MDA is designed to establish domain invariance at the micro level, a departure from the conventional category-level domain invariance. This shift alleviates the rigorous constraints associated with category-level domain invariance by concentrating on achieving invariance specifically among samples sharing similar semantics, eschewing unnecessary alignment of samples in one category with distant semantics. In practice, we pursue micro-level domain invariance by aligning features and their latent semantics across domains:

$$P_1^S(\Phi, S) = P_2^S(\Phi, S) = \dots = P_M^S(\Phi, S), \quad (6)$$

where S denotes the latent semantics of features, (Φ, S) represents the joint variable of Φ and S , and P_i^S refers to the corresponding distribution in source domain i .

The necessity for the latent semantics of features to possess the capability to discern subtle distinctions among samples within a single category is paramount for the success of micro-level alignment. In the absence of such discernment, deficient semantics may offer little assistance and, in certain cases, could even be detrimental to the alignment process, particularly when two distinct images share similar semantics. To address this challenge, we introduce a set of M additional specialist experts $\{E_i\}_{i=1}^M$, to model the latent feature semantics and thereby capture these subtle differences of samples in a certain category, each expert tailored to a specific source domain. In practice, we opt for a simplified approach, employing two fully connected layers for each expert to avoid the intricacies of more complex models. The dimension of the first layer output corresponds to the number of classes, enabling the optimization of semantic experts, while the dimension of the subsequent layer output matches that of the features. The optimization is achieved through the minimization of cross-entropy loss between the outputs in the first layer, denoted as $E_i^1(\Phi)$, and the ground truth:

$$\mathcal{L}_{exp} = \sum_{i=1}^M \sum_{x,y} P_i^S(x,y) \ell(E_i^1(\Phi), y). \quad (7)$$

In practical application, we utilize experts' outputs, denoted as $S = E_i(\Phi)$, as surrogates for latent semantics. The first layer outputs of experts preserve predictive scores of other categories, in contrast to ground-truth labels which omit information of other categories. The predicted class scores may exhibit variations even for samples within the same category. As a consequence, the predicted latent semantics S , based on the first layer outputs, is well-suited to capturing nuanced distinctions among samples in one category. Consequently,

they effectively meet the criteria necessary for feature latent semantics to facilitate micro-level alignment.

Micro-level Distribution Alignment vs. Category Alignment. It is of paramount importance to establish micro-level invariance based on experts' predicting semantics rather than enforcing category-level invariance solely relying on ground-truth labels across source domains. This necessity arises from the fact that attributes of different images within the same category may exhibit significant variations. Consequently, aligning class-to-class samples may emphasize invariant yet less significant features, potentially having an adverse effect on the acquisition of features with high generalizability and subsequently increasing empirical risk. In this way, category alignment may offer limited benefits and compromise classification accuracy. In contrast, the outputs of these experts encompass a spectrum of latent semantics across source domains, capable of reflecting various sample attributes in each class. Hence, these predicting outputs can be considered as the latent feature semantics for micro-level alignment. Consequently, MDA exhibits increased robustness to samples with significant variations and is more tolerant with within-class variations, thereby enhancing generalization performance.

In practice, we lack direct access to the semantic-based distributions $\{P_1^S(\Phi, S), P_2^S(\Phi, S), \dots, P_M^S(\Phi, S)\}$. This absence of access hinders our ability to match distributions across source domains. To tackle this challenge, we employ mutual information as a measure to assess the independence between the domain-dependent variables U and the semantic-based variables (Φ, S) . Consequently, we optimize the feature extractor by minimizing the mutual information:

$$\begin{aligned}
& \arg \min_f I(U; (\Phi, S)) \\
&= \arg \min_f \{H(U) - H(U|(\Phi, S))\} \\
&= \arg \min_f -H(U|(\Phi, S)) \\
&= \arg \min_f \mathbb{E}_{P^S(X, Y, U)} [\log P(U|(\Phi, S))] \\
&= \arg \min_f \mathbb{E}_{P^S(X, Y)} [\log P(U|(\Phi, S))],
\end{aligned} \tag{8}$$

where $P(U|(\Phi, S))$ represents the probability of U conditioned on the semantic-based variables (Φ, S) . It is worth noting that as domain-dependent variable U remains constant throughout the feature extractor optimization process, the first term $H(U)$ can be safely omitted from the objective. However, the unavailability of the distribution $P(U|(\Phi, S))$ still poses a challenge for minimization.

To facilitate the minimization, we introduce a distribution approximator D designed to approximate the conditional distribution as: $D(\Phi, S) := P(U|(\Phi, S))$. Given the intractability of the conditional distribution, we are unable to directly evaluate the quality of the function D . As a consequence, if the predictions of D are inaccurate, the mutual information minimization in Eq. (8) based on such predictions makes nonsense. In response, we reframe the minimization of the negative conditional entropy $-H(U|(\Phi, S))$ in Eq. (8) as a more challenging problem: optimizing the worst risk of mutual information by minimizing the supremum of the

Algorithm 1 Training algorithm for DG via DMDA

Input: M source training datasets: $\{S_i\}_{i=1}^M$
Parameter: Weighting factor: α, β , quantile parameter: m
Output: Feature extractor: f , semantics experts: $\{E_i\}_{i=1}^M$, classifiers: g, g_a , distribution approximator: D

- 1: **while** training is not converged **do**
- 2: **for** $i = 1$ to M **do**
- 3: Sample data from S_i
- 4: Generate the channel mask and prune the features
- 5: Calculate the latent semantics of pruned features
- 6: Sum the pruned features and the predicted latent semantics to surrogate the joint distributions
- 7: Update D by maximizing Eq. (13)
- 8: Update f, g, g_a , and E_i by minimizing Eq. (13)
- 9: **end for**
- 10: **end while**

approximated negative conditional entropy, where we denote $\mathbb{E}_{P^S(X, Y)} \log D(\Phi, S)$ as $-H(D(\Phi, S))$:

$$\min_f \sup_D \mathbb{E}_{P^S(X, Y)} \log D(\Phi, S). \tag{9}$$

Turning the intractable negative entropy $-H(U|(\Phi, S))$ into the supremum of the approximated negative conditional entropy $-H(D(\Phi, S))$ makes the optimization of Eq. (8) achievable. Considering that the range of D is closed, we employ the following minimax game to address Eq. (9):

$$\begin{aligned}
& \min_f \max_D \mathbb{E}_{P^S(X, Y)} \log D(\Phi, S) \\
&= \min_f \max_D \sum_{i=1}^M \sum_{x, y} P_i^S(x, y) \log D_i(\Phi, S) \\
&= \min_f \max_D \sum_{i=1}^M \sum_{x, y} P_i^S(x, y) \log D_i(\Phi, E_i(\Phi)).
\end{aligned} \tag{10}$$

The subsequent proposition and theory elucidate that the minimax game in Eq. (10) is equivalent to aligning the semantic-based distributions $P(\Phi, S)$ across source domains.

Proposition 1: Let $\Phi' = f(X)$ for a fixed representation function f and $S' = \{E_i(\Phi)\}_{i=1}^M$ for fixed semantics experts $\{E_i\}_{i=1}^M$, then the optimal probability D^* for the inner maximization in Eq. (10) is

$$D_i^*(\Phi', S') = \frac{P_i^S(\Phi', S')}{\sum_{j=1}^M P_j^S(\Phi', S')}. \tag{11}$$

The proof can be found in Sec. A of the appendix. Building upon Proposition 1, the ensuing theorem establishes the equivalence between the minimax game in Eq. (10) and the matching of semantic-based distributions across source domains in Eq. (6). The detailed proof is provided in Sec. B of the appendix.

Theorem 1: For a given representation function f , if U is the maximum of $-H(D(\Phi, S))$, i.e., $U = \sum_{i=1}^M \sum_{x, y} P_i^S(x, y) \log \frac{P_i^S(\Phi, S)}{\sum_{j=1}^M P_j^S(\Phi, S)}$. Then the solution of Eq. (10) can be achieved if and only if $P_1^S(\Phi, S) = P_2^S(\Phi, S) = \dots = P_M^S(\Phi, S)$.

TABLE I

GENERALIZATION PERFORMANCE WITH RECOGNITION ACCURACY (%) ON PACS [72] USING IMAGENET PRE-TRAINED RESNET-50. HIGHER IS BETTER, BOLD INDICATES THE BEST PERFORMANCE.

Method	Art	Cartoon	Photo	Sketch	Avg.(↑)
IRM [73]	84.8	76.4	96.7	76.1	83.5
GroupDRO [74]	83.5	79.1	96.7	78.3	84.4
Mixup [75]	86.1	78.9	97.6	75.8	84.6
MMD [44]	86.1	79.4	96.6	76.5	84.7
VREx [76]	86.0	79.1	96.9	77.7	84.9
RSC [77]	85.4	79.7	97.6	78.2	85.2
DANN [30]	86.4	77.4	97.3	73.5	83.7
CDANN [53]	85.0	78.9	98.1	76.4	84.6
MTL [78]	87.5	77.1	96.4	77.3	84.6
SagNet [79]	87.4	80.7	97.1	80.0	86.3
ARM [80]	86.8	76.8	97.4	79.3	85.1
SelfReg [†] [59]	87.9	79.4	96.8	78.3	85.6
PCL [†] [48]	87.3	77.5	96.3	83.2	86.1
AdaNPC [81]	87.1	82.2	97.5	81.5	87.1
FSR [17]	84.4	78.3	96.0	78.1	84.2
IPCL [58]	85.8	83.8	96.6	82.1	87.1
DMDA (ours)	87.1	85.2	96.7	83.5	88.1

Hence, the objective for matching the semantic-aware distributions across source domains can be formulated as:

$$\min_f \max_D \mathcal{L}_{MDA}, \quad (12)$$

with $\mathcal{L}_{MDA} = \mathbb{E}_{P^S(X,Y)} \log D(\Phi, S)$.

D. Optimization Objective

Together with the classification loss \mathcal{L}_{cla} , the overall objective function for our proposed DMDA is:

$$\min_{g, g_a, \{E_i\}_{i=1}^M} \max_{D, f} \mathcal{L}, \quad (13)$$

with $\mathcal{L} = \mathcal{L}_{cla} + \alpha \cdot (\mathcal{L}_{MDA} + \mathcal{L}_{exp}) + \beta \cdot \mathcal{L}_{aux}$,

where α and β represent the trade-off hyper-parameters. \mathcal{L}_{cla} , \mathcal{L}_{MDA} , \mathcal{L}_{exp} , and \mathcal{L}_{aux} denote the classification loss of the hypothesis model, semantic-aware invariance loss, semantics experts' accuracy loss, and the classification loss of the auxiliary classifier, respectively.

Micro-level Distributions. In practice, instead of simply concatenating features Φ and semantics S , we employ an element-wise summation of the acquired features and the semantics to construct a surrogate distribution. The idea of element-wise summation is inspired by the operation of position embeddings in Transformer [71], which has been demonstrated to be simple yet effective in embedding the information.

The pseudo-code is provided in Algorithm 1.

IV. EXPERIMENTS

In order to verify the efficiency of the proposed DMDA, we compare it with state-of-the-art approaches in DG, including Invariant Risk Minimization (IRM) [73], Group Distributionally Robust Optimization (GroupDRO) [74], Inter-domain Mixup (Mixup) [75], Maximum Mean Discrepancy (MMD) [44], Variance Risk Extrapolation (VREx) [76], Representation Self-Challenging (RSC) [77], Domain Adversarial Neural Network (DANN) [30], Conditional Domain Adversarial Neural Network (CDANN) [53], Marginal Transfer

TABLE II

GENERALIZATION PERFORMANCE WITH RECOGNITION ACCURACY (%) ON VLCS [83] USING IMAGENET PRE-TRAINED RESNET-50. HIGHER IS BETTER, BOLD INDICATES THE BEST PERFORMANCE.

Method	Caltech	LabelMe	SUN	VOC	Avg.(↑)
IRM [73]	98.6	64.9	73.4	77.3	78.5
GroupDRO [74]	97.3	63.4	69.5	76.7	76.7
Mixup [75]	98.3	64.8	72.1	74.3	77.4
MMD [44]	97.7	64.0	72.8	75.3	77.5
VREx [76]	98.4	64.4	74.1	76.2	78.3
RSC [77]	97.9	62.5	72.3	75.6	77.1
DANN [30]	99.0	65.1	73.1	77.2	78.6
CDANN [53]	97.1	65.1	70.7	77.1	77.5
MTL [78]	97.8	64.3	71.5	75.3	77.2
SagNet [79]	97.9	64.5	71.4	77.5	77.8
ARM [80]	98.7	63.6	71.3	76.7	77.6
SelfReg [†] [59]	96.7	65.2	73.1	76.2	77.8
PCL [†] [48]	96.6	58.1	72.4	75.2	75.6
AdaNPC [81]	98.9	64.5	73.5	75.6	78.1
FSR [17]	89.6	64.1	70.8	75.0	74.9
IPCL [58]	97.7	63.8	73.8	78.1	78.4
DMDA (ours)	98.2	64.3	74.4	80.8	79.4

Learning (MTL) [78], Style Agnostic Networks (SagNet) [79], Adaptive Risk Minimization (ARM) [80], Self-supervised contrastive Regularization (SelfReg) [59], Proxy-based Contrastive Learning (PCL) [48], Non-Parametric Classifier for test-time Adaptation (AdaNPC) [81], Feature-based Style Randomization (FSR) [17], and Instance Paradigm Contrastive Learning (IPCL) [58]. The performances of those models are from the original literature or DomainBed [82]. While [†] in the tables means the reproduced results without the ensembling technique for a fair comparison.

A. Datasets

Following previous DG protocols [42], [59], [69], [82], we validate our proposed methods on five widely-used datasets: (1) **PACS** [72] comprises four distinct domains: Photo, Art, Cartoon, and Sketch, with each domain encompassing seven classes. (2) **VLCS** [83] contains four standard datasets: Caltech [84], LabelMe [85], SUN [86], and VOC [87]. In each dataset, there are five categories: bird, car, chair, dog, and person. (3) **OfficeHome** [88] consists of four diverse domains: Art, Clipart, Product, and Real-World, each containing 65 classes. (4) **TerraIncognita** [23] showcases photographs of wild animals captured at various locations: L100, L38, L43, and L46, each of which includes 10 classes. (5) **DomainNet** [89] constitutes a substantial dataset, encompassing 586,575 images across six domains, with each domain comprising 345 classes.

B. Implementation Details

Adhering to established DG protocols [69], [82], we employ ImageNet [90] pre-trained ResNet-50 [2] as the backbone, with the last FC layer serving as the label predictor and the preceding layers functioning as the feature extractor. We utilize three FC layers to construct the distribution approximator which receives inputs through a gradient reverse layer (GRL) [30], and the output dimensions are 256, 256, and the number of source domains, respectively. Our model undergoes training

TABLE III

GENERALIZATION PERFORMANCE WITH RECOGNITION ACCURACY (%) ON OFFICEHOME [88] USING IMAGENET PRE-TRAINED RESNET-50. HIGHER IS BETTER, BOLD INDICATES THE BEST PERFORMANCE.

Method	Art	Clipart	Product	Real-World	Avg.(↑)
IRM [73]	58.9	52.2	72.1	74.0	64.3
GroupDRO [74]	60.4	52.7	75.0	76.0	66.0
Mixup [75]	62.4	54.8	76.9	78.3	68.1
MMD [44]	60.4	53.3	74.3	77.4	66.4
VREx [76]	60.7	53.0	75.3	76.7	66.4
RSC [77]	60.7	51.4	74.8	75.1	65.5
DANN [30]	59.9	53.0	73.6	76.9	65.9
CDANN [53]	61.5	50.4	74.4	76.6	65.7
MTL [78]	61.5	52.4	74.9	76.8	66.4
SagNet [79]	63.4	54.8	75.8	78.3	68.1
ARM [80]	58.9	51.0	74.1	75.2	64.8
SelfReg [†] [59]	63.6	53.1	76.9	78.1	67.9
PCL [†] [48]	62.7	54.0	76.9	78.5	68.0
AdaNPC [81]	62.9	52.3	75.1	75.6	66.5
FSR [17]	59.7	55.9	74.7	74.9	66.3
IPCL [58]	65.1	56.8	77.3	77.1	69.1
DMDA (ours)	66.1	56.1	77.3	77.9	69.4

TABLE IV

HYPERPARAMETER SEARCH SPACE, WITH $m = q/100$.

Hyperparameter	Search space
α	[1]
β	[3, 5]
m	[0.5, 0.4, 0.3]
learning rate	[1e-3, 5e-4]

for 15k iterations for DomainNet and 5k iterations for others, utilizing SGD with a momentum of 0.9, weight decay set to $5e-4$. The learning rate is decayed by a factor of 0.1 at 70% and 90% of the total epochs. The batch size is fixed at 32 for each domain. The adaptation parameter in GRL is initialized at 0 and gradually transitions to 1 following [30]. For additional hyperparameter details, please refer to TABLE IV.

To ensure a fair comparison, we adhere to the training-domain validation evaluation protocol following DomainBed [82]. This entails cyclically selecting one domain as the target domain, with the remaining domains serving as source domains. Within each source domain, we execute an 80%/20% train/validation partition, whereby the validation portions across all source domains collectively compose the validation dataset used for model validation and selection.

C. Comparison Results with State-of-the-Art Techniques

The results on PACS are presented in TABLE I. While our approach may not consistently achieve the highest accuracy in specific scenarios, it demonstrates significant improvements across most scenarios. Moreover, the highest average object recognition accuracy which outperforms the SOTA method IPCL by 1.1% attests to the efficacy of DMDA for DG. Notably, DMDA excels in enhancing the generalization performance in hard-to-transfer domains where style markedly diverges from the other domains. It exhibits a notable superiority of 1.7% on ‘Cartoon’ and 1.3% on ‘Sketch’ compared to IPCL. This observation underscores DMDA’s capacity to

TABLE V

GENERALIZATION PERFORMANCE ON TERRAINCOGNITA [23] USING IMAGENET PRE-TRAINED RESNET-50. HIGHER IS BETTER, BOLD INDICATES THE BEST PERFORMANCE OUT OF ALL COMPARED METHODS.

Method	L100	L38	L43	L46	Avg.(↑)
IRM [73]	54.6	39.8	56.2	39.6	47.6
GroupDRO [74]	41.2	38.6	56.7	36.4	43.2
Mixup [75]	59.6	42.2	55.9	33.9	47.9
MMD [44]	41.9	34.8	57.0	35.2	42.2
VREx [76]	48.2	41.7	56.8	38.7	46.4
RSC [77]	50.2	39.2	56.3	40.8	46.6
DANN [30]	51.1	40.6	57.4	37.7	46.7
CDANN [53]	47.0	41.3	54.9	39.8	45.8
MTL [78]	49.3	39.6	55.6	37.8	45.6
SagNet [79]	53.0	43.0	57.9	40.4	48.6
ARM [80]	49.3	38.3	55.8	38.7	45.5
SelfReg [†] [59]	48.8	41.3	57.3	40.6	47.0
PCL [†] [48]	41.6	42.8	52.9	40.1	44.3
AdaNPC [81]	56.7	48.5	47.5	35.4	47.0
FSR [17]	57.4	37.8	54.8	36.1	46.5
IPCL [58]	50.9	41.3	54.6	40.6	46.8
DMDA (ours)	55.9	41.7	56.8	43.6	49.5

TABLE VI

GENERALIZATION PERFORMANCE ON DOMAINNET [89] USING IMAGENET PRE-TRAINED RESNET-50. HIGHER IS BETTER, BOLD INDICATES THE BEST PERFORMANCE OUT OF ALL COMPARED METHODS.

Method	Clipart	Infograph	Painting	Quickdraw	Real Sketch	Avg.(↑)
IRM [70]	48.5	15.0	38.3	10.9	48.2	42.3
GroupDRO [71]	47.2	17.5	33.8	9.3	51.6	40.1
Mixup [72]	55.7	18.5	44.3	12.5	55.8	48.2
MMD [44]	32.1	11.0	26.8	8.7	32.7	28.9
VREx [73]	47.3	16.0	35.8	10.9	49.6	42.0
RSC [74]	55.0	18.3	44.4	12.2	55.7	47.8
DANN [30]	53.1	18.3	44.2	11.8	55.5	46.8
CDANN [52]	54.6	17.3	43.7	12.1	56.2	45.9
MTL [75]	57.9	18.5	46.0	12.5	59.5	49.2
SagNet [76]	57.7	19.0	45.3	12.7	58.1	48.8
ARM [77]	49.7	16.3	40.9	9.4	53.4	43.5
SelfReg [†] [57]	60.7	21.6	49.4	12.7	60.7	51.7
PCL [†] [48]	62.5	21.1	49.5	14.1	61.3	51.8
AdaNPC [78]	59.3	22.2	48.3	14.3	61.0	51.4
FSR [17]	59.0	18.2	46.7	15.0	55.8	49.5
IPCL [58]	55.3	18.6	39.4	11.9	64.7	53.9
DMDA (ours)	65.8	22.5	51.9	15.5	64.2	54.7

cultivate superior representations for effective generalization to novel environments.

TABLE II reports the outcomes for VLCS. DMDA achieves the best average generalization performance and demonstrates substantial improvements across most scenarios when compared to alternative methods. Additionally, in hard-to-transfer domains, DMDA outperforms the SOTA method DANN by 4.7% on ‘VOC’ and 1.8% on ‘SUN’. This outcome underscores the superior efficacy of DMDA, even in the face of the heightened generalization challenges posed by scene-centric images within VLCS.

The generalization performances for OfficeHome are detailed in TABLE III. DMDA consistently demonstrates superior performance in the majority of scenarios, along with achieving the highest average object recognition accuracy. A remarkable aspect of DMDA is its substantial performance enhancement in hard-to-transfer domains like ‘Art’ and ‘Clipart’. This notable improvement underscores the validity of our

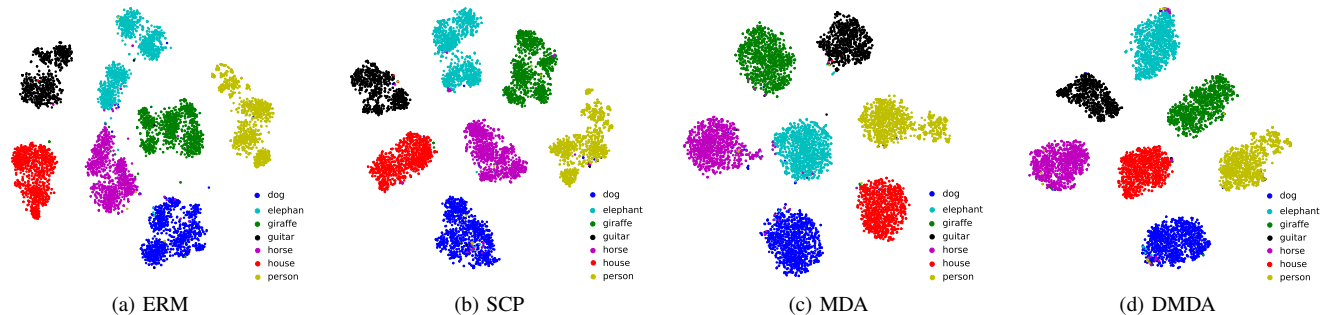


Fig. 5. Visualizations with t-SNE embeddings [91] depicting distinct classes' representations produced by (a) ERM, (b) SCP, (c) MDA, and (d) the combination DMDA, respectively, with 'Photo' as the target domain. Zoom in for details.

TABLE VII

ABLATION STUDY OF THE OUR DMDA ON DIVERSE BENCHMARKS. HIGHER IS BETTER, BOLD INDICATES THE BEST PERFORMANCE.

Method	PACS	VLCS	OfficeHome	TerraIncognita	DomainNet
ERM	85.5	77.5	66.5	46.1	43.0
w/ SCP	86.7	78.4	68.7	48.5	45.1
w/ MDA	86.9	78.6	67.7	48.9	44.2
DMDA (ours)	88.1	79.4	69.4	49.5	45.8

TABLE VIII

COMPARISON BETWEEN DROPOUT [92] AND SCP ON DIVERSE BENCHMARKS. HIGHER IS BETTER, BOLD INDICATES THE BEST PERFORMANCE.

Method	PACS	VLCS	OfficeHome	TerraIncognita	DomainNet
Dropout [92]	84.9	78.3	64.8	47.4	43.7
SCP (ours)	88.1	79.4	69.4	49.5	45.8

approach, which strives to cultivate improved representations characterized by superior discriminability and generalizability.

TABLE V displays the findings of TerraIncognita. DMDA outperforms state-of-the-art methods in terms of average object recognition accuracy. Furthermore, our model exhibits a significant improvement of 7.9% compared to the SOTA method in the most challenging scenario, namely, the 'L46' domain. This observation highlights the inherent capability of our method to acquire discriminative representations across domains.

The outcomes on the more challenging benchmark, DomainNet, are documented in TABLE VI, demonstrating the superior generalization performance of our proposed DMDA in five out of six scenarios. Furthermore, DMDA surpasses the state-of-the-art method PCL by 5.5% in terms of average generalization performance. These results substantiate our assertion that the proposed DMDA has the potential to enhance both feature discriminability and discriminability.

D. Ablation Study

Effectiveness of Each Component. We undertake ablation studies on five benchmarks to assess the individual effectiveness of SCP and MDA. TABLE VII presents the generalization performance as we incrementally integrate SCP and MDA into ERM. As can be observed, both SCP and MDA contribute positively to enhanced generalization capabilities. The optimal performance is realized when SCP and MDA are combined,

TABLE IX

INTEGRATION OF SCP WITH DISTRIBUTION MATCHING METHODS ON PACS. HIGHER IS BETTER, BOLD INDICATES THE BEST PERFORMANCE.

Method	Art	Cartoon	Photo	Sketch	Avg.(↑)
DANN [30]	86.4	77.4	97.3	73.5	83.7
w/ SCP	87.0	83.0	96.9	76.0	85.7
CDANN [53]	85.0	78.9	98.1	76.4	84.6
w/ SCP	87.4	83.2	96.6	78.3	86.4
ER [39]	87.5	79.3	98.3	76.3	85.3
w/ SCP	87.5	81.5	97.8	80.2	86.8
MDA (ours)	87.3	81.5	96.8	82.1	86.9
w/ SCP	87.1	85.2	96.7	83.5	88.1

underscoring the indispensability of both SCP and MDA in improving generalization performance.

The t-SNE Visualization of Features. With the collaborative integration of SCP and MDA, the learned features exhibit the superiority of both high discriminability and generalizability. Fig. 5 depicts the t-SNE embeddings of the learned features with ERM, SCP, MDA, and the cooperation DMDA, respectively. As observed, both SCP and MDA manifest superior representations in comparison to ERM. Moreover, the cooperation exhibits better representations with heightened intra-class compactness in comparison to SCP and superior inter-class separation compared to MDA, demonstrating the necessity of both SCP and MDA.

E. Empirical Analysis

In this section, we conduct empirical analysis to investigate the impact of different modules in DMDA and compare it with existing distribution matching methods to assess the effectiveness of our method. The analysis aims to shed light on the reasons behind our approach's strong performance.

Comparison with Dropout. Our proposed SCP endeavors to prune inconsistent channels across domains, aiming to eliminate spurious correlations rather than merely mitigating the interdependence among neurons akin to Dropout. To substantiate the effectiveness of SCP in eliminating spurious correlations, experiments were undertaken on various benchmarks utilizing both Dropout [92] and our novel SCP. The outcomes, as illustrated in TABLE VIII, reveal a notable improvement in the generalization performance of SCP by 2.1%, 0.1%, 6.0%, 2.3%, and 3.2% on PACS, VLCS, OfficeHome, TerraIncognita and DomainNet, respectively. These consistent findings

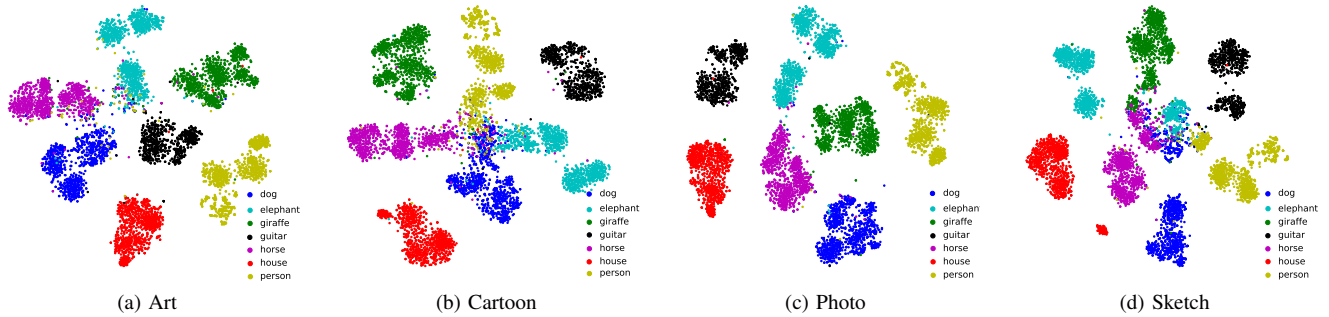


Fig. 6. Visualizations with t-SNE embeddings [91] depicting representations of distinct classes of ERM, where (a) Art, (b) Cartoon, (c) Photo, and (d) Sketch are individually selected as the target domain. Zoom in for details.

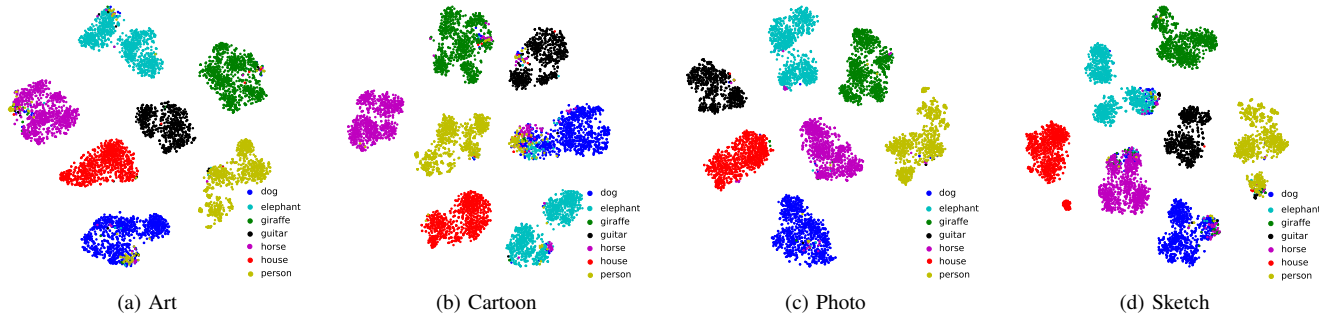


Fig. 7. Visualizations using t-SNE embeddings [91] representing features of SCP-based ERM, with (a) Art, (b) Cartoon, (c) Photo, and (d) Sketch individually chosen as the target domain. The pruned features exhibit a clustering effect. Zoom in for details.

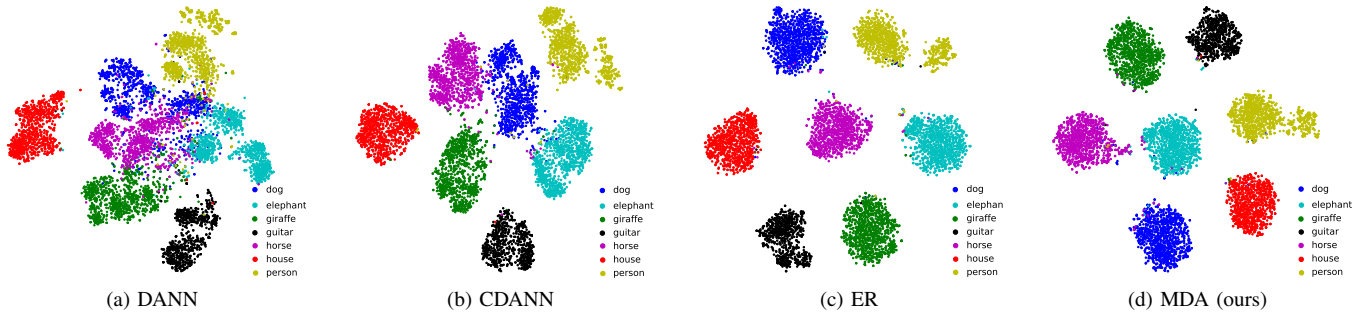


Fig. 8. Visualizations with t-SNE embeddings [91] illustrating various classes' representations produced by (a) DANN [30], (b) CDANN [53], (c) ER [39], and (d) MDA (ours), respectively. MDA demonstrates the superior clustering effect. Zoom in for details.

consistently affirm the superior ability of SCP to eliminate spurious features, thereby enhancing feature discriminability.

Feature Visualization with SCP. To visually evaluate the efficacy of the proposed SCP, we visualize the acquired features with t-SNE embeddings [91]. Specifically, we conduct experiments on PACS and take each domain as the target domain in turn. The clustering results, based on the features generated by ERM and SCP-based ERM, are depicted in Fig. 6 and Fig. 7, respectively. Evidently, the introduced SCP module consistently improves the representation learning across all scenarios. The observed high inter-class separation and intra-class compactness in all scenarios further affirm the superiority of SCP for enhancing feature discriminability.

Integration into Distribution Matching Models. To further assess the effectiveness of SCP in enhancing feature

discriminability, we integrate SCP with distribution matching models, namely DANN [30], CDANN [53], ER [39], and the proposed MDA. In our integration, we refrain from fine-tuning and maintain the same hyperparameters of these distribution matching techniques. This restraint underscores the robustness of SCP's effectiveness. The corresponding generalization performances are presented in TABLE IX. The results indicate that SCP significantly enhances the generalization performance of these distribution matching methods, particularly in hard-to-transfer domains. These observations reinforce the superior capabilities of SCP in improving feature discriminability.

Comparison with Existing Distribution Matching Models. To demonstrate the superiority of the proposed MDA over existing distribution matching models, we conduct experiments

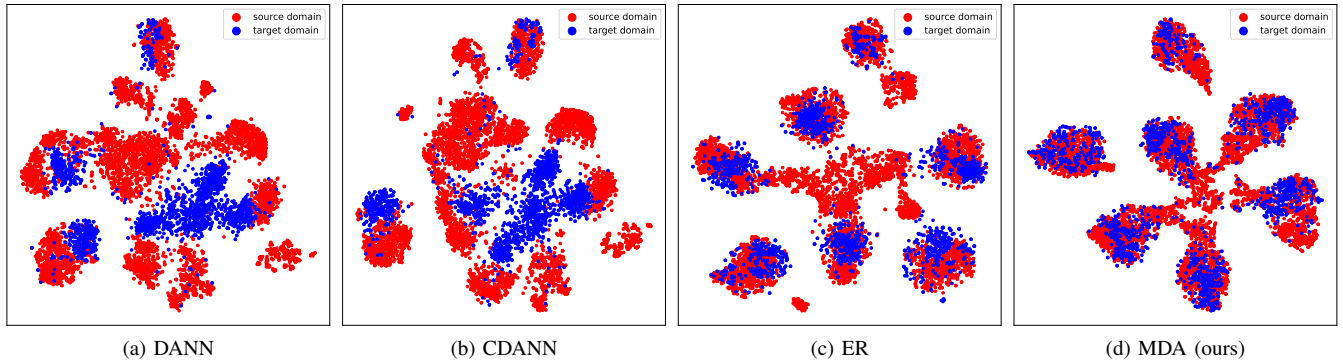


Fig. 9. Visualizations with t-SNE embeddings [91] for the representations across source domain and target domain learned by (a) DANN [30], (b) CDANN [53], (c) ER [39], and (d) MDA, respectively. The distribution discrepancy of MDA is the smallest.

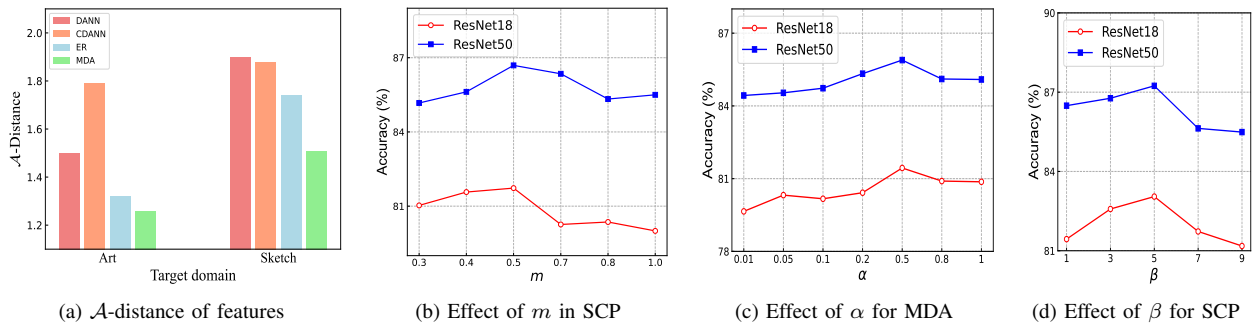


Fig. 10. (a) \mathcal{A} -distance of features learned by DANN, CDANN, ER, and the proposed MDA, respectively. Lower is better. (b) Generalization performance of SCP w.r.t. the quantile m . (c) Generalization performance of MDA w.r.t. the hyperparameter α . (d) Performance of SCP w.r.t. the coefficient β .

TABLE X
COMPARISON OF DISTRIBUTION MATCHING MODELS WITH DISTINCT BACKBONES ON PACS. BOLD INDICATES THE BEST PERFORMANCE.

Method	Art	Cartoon	Photo	Sketch	Avg.(\uparrow)
ResNet-18					
DANN [30]	77.4	66.8	96.6	69.8	77.7
CDANN [53]	75.2	74.0	95.7	72.9	79.4
ER [39]	80.7	76.4	96.7	71.8	81.4
MDA (ours)	81.0	78.5	95.5	77.4	83.1
ResNet-50					
DANN [30]	86.4	77.4	97.3	73.5	83.7
CDANN [53]	85.0	78.9	98.1	76.4	84.6
ER [39]	87.5	79.3	98.3	76.3	85.3
MDA (ours)	87.3	81.5	96.8	82.1	86.9

on PACS using DANN [30], CDANN [53], ER [39], and MDA, respectively. The results, obtained with various backbones, as shown in TABLE X, consistently affirm MDA’s superiority in terms of generalization performance. Particularly noteworthy is MDA’s substantial enhancement in hard-to-transfer domains such as ‘Cartoon’ and ‘Sketch’, where other distribution matching methods struggle significantly.

Feature Visualization with MDA. To visually illustrate the impact of MDA, we employ t-SNE embeddings to visualize the acquired features. Specifically, we take experiments on PACS, with ‘Photo’ as the target domain. Fig. 8 depicts the clustering results based on the features generated by DANN [30], CDANN [53], ER [39], and the proposed MDA, respectively. Notably, MDA demonstrates superior representa-

tions characterized by high inter-class separation and intra-class compactness, particularly when compared to DANN and CDANN. While the improvement over ER may not be pronounced, notably observations can still be made. Firstly, the clustering of ‘guitar’ (black) and ‘person’ (yellow) is noticeably more compact with MDA. Secondly, the peripheries of class clusters exhibit greater dispersion with ER, highlighting the better representation achieved by the proposed MDA.

Distribution Discrepancy. To assess the impact of MDA on domain invariance, we employ the \mathcal{A} -distance as a metric to gauge the distribution divergence across domains [93]. A proxy \mathcal{A} -distance can be defined as $d_{\mathcal{A}} = 2(1 - 2\sigma)$, where σ represents the error of a binary discriminator in correctly distinguishing between source and target domain samples. In our case, the discriminator is implemented as a neural network with a single FC layer. As shown in Fig. 10a, MDA achieves a representation space characterized by a smaller domain discrepancy when compared to other distribution matching approaches. We further present t-SNE embeddings [91] of the acquired features from source domains and target domain in Fig. 9. Notably, it is evident that the distributions of the acquired features across the source domain and target domain, when MDA is employed, exhibit a closer alignment. This observation substantiates MDA’s capacity to learn features with enhanced generalizability, surpassing the capabilities of DANN [30], CDANN [53] and ER [39].

Hyperparameter Influence. We explore the influence of the quantile parameter m in SCP, trade-off parameter α for

MDA and β for SCP on the generalization performance. Fig. 10b, Fig. 10c and Fig. 10d illustrate the generalization accuracies of SCP and MDA, utilizing two different pre-trained backbones, ResNet-18 and ResNet-50. We systematically vary m within the range $\{0.3, 0.4, 0.5, 0.7, 0.8, 1.0\}$, α within the range $\{0.01, 0.05, 0.1, 0.2, 0.5, 0.8, 1.0\}$, and β within the range $\{1, 3, 5, 7, 9\}$. The consistent trend of initially increasing and subsequently decreasing generalization performance observed in both SCP and MDA underscores their vital role in enhancing generalization performance. For the selected trade-off values in the overall objectives, we consistently set α to 1.0 throughout all experiments to ensure the effectiveness of MDA, while employing β values of 3 and 5 consistently across all experiments, thereby underscoring the robustness of our proposed modules. Subsequently, we select the optimal experimental outcome from these options of β .

V. CONCLUSION

In this paper, we present a novel perspective on DG by concurrently enhancing feature generalizability while elevating feature discriminability. We introduce a novel framework for domain-invariant representation learning, named Discriminative Microscopic Distribution Alignment (DMDA), comprising two key modules: Selective Channel Pruning (CAP) and Micro-level Distribution Alignment (MDA). SCP is designed to enhance feature discriminability by eliminating spurious correlations within neural networks. It achieves this by selectively pruning unstable channels. On the other hand, MDA attempts to excavate sufficient generalizable features while accommodating within-class variations through a micro-level alignment manner. Experiments on four benchmark datasets demonstrate the efficacy of DMDA in learning an increased representation space characterized by superior discriminability and generalizability, thereby leading to improved generalization performance. Our proposed method sheds light on the significance of stable factors and micro-level alignment in domain-invariant representation learning for DG.

REFERENCES

- [1] A. Krizhevsky, I. Sutskever, and G. E. Hinton, "Imagenet classification with deep convolutional neural networks," in *Proceedings of the Advances in Neural Information Processing Systems*, 2012, pp. 84–90.
- [2] K. He, X. Zhang, S. Ren, and J. Sun, "Deep residual learning for image recognition," in *Proceedings of the IEEE/CVF Conference on Computer Vision and Pattern Recognition*, 2016, pp. 770–778.
- [3] A. Dosovitskiy, L. Beyer, A. Kolesnikov, D. Weissenborn, X. Zhai, T. Unterthiner, M. Dehghani, M. Minderer, G. Heigold, S. Gelly, J. Uszkoreit, and N. Houlsby, "An image is worth 16x16 words: Transformers for image recognition at scale," in *International Conference on Learning Representations*, 2020.
- [4] Z. Feng, Q. Zhou, Q. Gu, X. Tan, G. Cheng, X. Lu, J. Shi, and L. Ma, "Dmt: Dynamic mutual training for semi-supervised learning," *Pattern Recognition*, vol. 130, p. 108777, 2022.
- [5] Y. Song, Q. Zhou, and L. Ma, "Rethinking implicit neural representations for vision learners," in *Proceedings of the IEEE International Conference on Acoustics, Speech and Signal Processing*, 2023, pp. 1–5.
- [6] J. Long, E. Shelhamer, and T. Darrell, "Fully convolutional networks for semantic segmentation," in *Proceedings of the IEEE conference on computer vision and pattern recognition*, 2015, pp. 3431–3440.
- [7] O. Ronneberger, P. Fischer, and T. Brox, "U-net: Convolutional networks for biomedical image segmentation," in *Proceedings of the Medical Image Computing and Computer-Assisted Intervention*, 2015, pp. 234–241.
- [8] L.-C. Chen, Y. Zhu, G. Papandreou, F. Schroff, and H. Adam, "Encoder-decoder with atrous separable convolution for semantic image segmentation," in *Proceedings of the European conference on computer vision*, 2018, pp. 801–818.
- [9] S. Ren, K. He, R. Girshick, and J. Sun, "Faster r-cnn: Towards real-time object detection with region proposal networks," *Proceedings of the Advances in Neural Information Processing Systems*, pp. 91–99, 2015.
- [10] T.-Y. Lin, P. Dollár, R. Girshick, K. He, B. Hariharan, and S. Belongie, "Feature pyramid networks for object detection," in *Proceedings of the IEEE/CVF conference on computer vision and pattern recognition*, 2017, pp. 2117–2125.
- [11] J. Redmon, S. Divvala, R. Girshick, and A. Farhadi, "You only look once: Unified, real-time object detection," in *Proceedings of the IEEE/CVF conference on computer vision and pattern recognition*, 2016, pp. 779–788.
- [12] Q. Zhou, X. Li, L. He, Y. Yang, G. Cheng, Y. Tong, L. Ma, and D. Tao, "Transvod: end-to-end video object detection with spatial-temporal transformers," *IEEE Transactions on Pattern Analysis and Machine Intelligence*, vol. 45, no. 6, pp. 7853–7869, 2023.
- [13] L. He, Q. Zhou, X. Li, L. Niu, G. Cheng, X. Li, W. Liu, Y. Tong, L. Ma, and L. Zhang, "End-to-end video object detection with spatial-temporal transformers," in *Proceedings of the ACM International Conference on Multimedia*, 2021, pp. 1507–1516.
- [14] A. Li and J. Pearl, "Bounds on causal effects and application to high dimensional data," in *Proceedings of the AAAI Conference on Artificial Intelligence*, 2022, pp. 5773–5780.
- [15] R. Perry, J. von Kügelgen*, and B. Schölkopf*, "Causal discovery in heterogeneous environments under the sparse mechanism shift hypothesis," in *Proceedings of the Advances in Neural Information Processing Systems*, 2022, pp. 10904–10917.
- [16] T. Fang, N. Lu, G. Niu, and M. Sugiyama, "Rethinking importance weighting for deep learning under distribution shift," *Proceedings of the Advances in Neural Information Processing Systems*, pp. 11996–12007, 2020.
- [17] Y. Wang, L. Qi, Y. Shi, and Y. Gao, "Feature-based style randomization for domain generalization," *IEEE Transactions on Circuits and Systems for Video Technology*, vol. 32, no. 8, pp. 5495–5509, 2022.
- [18] Q. Tian, Y. Zhu, H. Sun, S. Chen, and H. Yin, "Unsupervised domain adaptation through dynamically aligning both the feature and label spaces," *IEEE Transactions on Circuits and Systems for Video Technology*, vol. 32, no. 12, pp. 8562–8573, 2022.
- [19] Q. Zhou, Z. Feng, Q. Gu, J. Pang, G. Cheng, X. Lu, J. Shi, and L. Ma, "Context-aware mixup for domain adaptive semantic segmentation," *IEEE Transactions on Circuits and Systems for Video Technology*, vol. 33, no. 2, pp. 804–817, 2022.
- [20] Y. Ren, Y. Cong, J. Dong, and G. Sun, "Uni3da: Universal 3d domain adaptation for object recognition," *IEEE Transactions on Circuits and Systems for Video Technology*, vol. 33, no. 1, pp. 379–392, 2022.
- [21] D. Hendrycks and T. Dietterich, "Benchmarking neural network robustness to common corruptions and perturbations," in *International Conference on Learning Representations*, 2018.
- [22] R. Taori, A. Dave, V. Shankar, N. Carlini, B. Recht, and L. Schmidt, "Measuring robustness to natural distribution shifts in image classification," in *Proceedings of the Advances in Neural Information Processing Systems*, 2020, pp. 18583–18599.
- [23] S. Beery, G. Van Horn, and P. Perona, "Recognition in terra incognita," in *Proceedings of the Proceedings of the European Conference on Computer Vision*, 2018, pp. 456–473.
- [24] B. Schölkopf, F. Locatello, S. Bauer, N. R. Ke, N. Kalchbrenner, A. Goyal, and Y. Bengio, "Towards causal representation learning," *arXiv preprint arXiv:2102.11107*, 2021.
- [25] Q. Gu, Q. Zhou, M. Xu, Z. Feng, G. Cheng, X. Lu, J. Shi, and L. Ma, "Pit: Position-invariant transform for cross-fov domain adaptation," in *Proceedings of the IEEE/CVF International Conference on Computer Vision*, 2021, pp. 8761–8770.
- [26] H. Fu, M. Gong, C. Wang, K. Batmanghelich, K. Zhang, and D. Tao, "Geometry-consistent generative adversarial networks for one-sided unsupervised domain mapping," in *Proceedings of the IEEE/CVF Conference on Computer Vision and Pattern Recognition*, 2019, pp. 2427–2436.
- [27] J. Pearl, "A probabilistic calculus of actions," *arXiv preprint arXiv:1302.6835*, 2013.
- [28] Y. Wei, L. Yang, Y. Han, and Q. Hu, "Multi-source collaborative contrastive learning for decentralized domain adaptation," *IEEE Transactions on Circuits and Systems for Video Technology*, vol. 33, no. 5, pp. 2202–2216, 2022.
- [29] R. Meng, X. Li, W. Chen, S. Yang, J. Song, X. Wang, L. Zhang, M. Song, D. Xie, and S. Pu, "Attention diversification for domain

- generalization,” in *Proceedings of the European conference on computer vision*, 2022, pp. 322–340.
- [30] Y. Ganin, E. Ustinova, H. Ajakan, P. Germain, H. Larochelle, F. Laviolette, M. March, and V. Lempitsky, “Domain-adversarial training of neural networks,” *Journal of Machine Learning Research*, vol. 17, no. 59, pp. 1–35, 2016.
- [31] K. Zhang, M. Gong, P. Stojanov, B. Huang, Q. Liu, and C. Glymour, “Domain Adaptation as a Problem of Inference on Graphical Models,” in *Proceedings of the Advances in Neural Information Processing Systems*, 2020, pp. 4965–4976.
- [32] Y. Zuo, H. Yao, L. Zhuang, and C. Xu, “Margin-based adversarial joint alignment domain adaptation,” *IEEE Transactions on Circuits and Systems for Video Technology*, vol. 32, no. 4, pp. 2057–2067, 2021.
- [33] Q. Zhou, K.-Y. Zhang, T. Yao, R. Yi, K. Sheng, S. Ding, and L. Ma, “Generative domain adaptation for face anti-spoofing,” in *Proceedings of the European conference on computer vision*, 2022, pp. 335–356.
- [34] Q. Zhou, Z. Feng, Q. Gu, G. Cheng, X. Lu, J. Shi, and L. Ma, “Uncertainty-aware consistency regularization for cross-domain semantic segmentation,” *Computer Vision and Image Understanding*, vol. 221, p. 103448, 2022.
- [35] Q. Zhou, C. Zhuang, R. Yi, X. Lu, and L. Ma, “Domain adaptive semantic segmentation via regional contrastive consistency regularization,” in *Proceedings of the IEEE International Conference on Multimedia and Expo*, 2022, pp. 01–06.
- [36] Q. Zhou, Q. Gu, J. Pang, X. Lu, and L. Ma, “Self-adversarial disentangling for specific domain adaptation,” *IEEE Transactions on Pattern Analysis and Machine Intelligence*, vol. 45, no. 7, pp. 8954–8968, 2023.
- [37] K. Muandet, D. Balduzzi, and B. Schölkopf, “Domain Generalization via Invariant Feature Representation,” in *Proceedings of the International Conference on Machine Learning*, 2013, pp. 10–18.
- [38] Y. Li, M. Gong, X. Tian, T. Liu, and D. Tao, “Domain generalization via conditional invariant representations,” in *Proceedings of the AAAI Conference on Artificial Intelligence*, 2018, pp. 3579–3587.
- [39] S. Zhao, M. Gong, T. Liu, H. Fu, and D. Tao, “Domain generalization via entropy regularization,” in *Proceedings of the Advances in Neural Information Processing Systems*, 2020, pp. 16 096–16 107.
- [40] Q. Zhou, K.-Y. Zhang, T. Yao, X. Lu, R. Yi, S. Ding, and L. Ma, “Instance-aware domain generalization for face anti-spoofing,” in *Proceedings of the IEEE/CVF Conference on Computer Vision and Pattern Recognition*, 2023, pp. 20 453–20 463.
- [41] Y. Zhao, Z. Zhong, N. Zhao, N. Sebe, and G. H. Lee, “Style-hallucinated dual consistency learning for domain generalized semantic segmentation,” in *Proceedings of the European conference on computer vision*, 2022, pp. 535–552.
- [42] B. Li, Y. Shen, J. Yang, Y. Wang, J. Ren, T. Che, J. Zhang, and Z. Liu, “Sparse mixture-of-experts are domain generalizable learners,” in *International Conference on Learning Representations*, 2023.
- [43] S. Motiian, M. Piccirilli, D. A. Adjeroh, and G. Doretto, “Unified deep supervised domain adaptation and generalization,” in *Proceedings of the IEEE/CVF international conference on computer vision*, 2017, pp. 5715–5725.
- [44] H. Li, S. J. Pan, S. Wang, and A. C. Kot, “Domain generalization with adversarial feature learning,” in *Proceedings of the IEEE/CVF conference on computer vision and pattern recognition*, 2018, pp. 5400–5409.
- [45] B. Sun and K. Saenko, “Deep coral: Correlation alignment for deep domain adaptation,” in *Proceedings of the European conference on computer vision*, 2016, pp. 443–450.
- [46] S. Li, B. Xie, J. Wu, Y. Zhao, C. H. Liu, and Z. Ding, “Simultaneous semantic alignment network for heterogeneous domain adaptation,” in *Proceedings of the ACM international conference on multimedia*, 2020, pp. 3866–3874.
- [47] Y. Zhao, S. Li, R. Zhang, C. H. Liu, W. Cao, X. Wang, and S. Tian, “Semantic correlation transfer for heterogeneous domain adaptation,” *IEEE Transactions on Neural Networks and Learning Systems*, pp. 1–13, 2022.
- [48] X. Yao, Y. Bai, X. Zhang, Y. Zhang, Q. Sun, R. Chen, R. Li, and B. Yu, “PcI: Proxy-based contrastive learning for domain generalization,” in *Proceedings of the IEEE/CVF Conference on Computer Vision and Pattern Recognition*, 2022, pp. 7097–7107.
- [49] H. Zhang, Y.-F. Zhang, W. Liu, A. Weller, B. Schölkopf, and E. P. Xing, “Towards principled disentanglement for domain generalization,” in *Proceedings of the IEEE/CVF Conference on Computer Vision and Pattern Recognition*, 2022, pp. 8024–8034.
- [50] D. Mahajan, S. Tople, and A. Sharma, “Domain generalization using causal matching,” in *Proceedings of the International Conference on Machine Learning*, 2021, pp. 7313–7324.
- [51] M. Ghifary, D. Balduzzi, W. B. Kleijn, and M. Zhang, “Scatter component analysis: A unified framework for domain adaptation and domain generalization,” *IEEE transactions on pattern analysis and machine intelligence*, vol. 39, no. 7, pp. 1414–1430, 2016.
- [52] Z. Gao, S. Guo, C. Xu, J. Zhang, M. Gong, J. Del Ser, and S. Li, “Multi-domain adversarial variational bayesian inference for domain generalization,” *IEEE Transactions on Circuits and Systems for Video Technology*, pp. 1–1, 2022.
- [53] Y. Li, X. Tian, M. Gong, Y. Liu, T. Liu, K. Zhang, and D. Tao, “Deep domain generalization via conditional invariant adversarial networks,” in *Proceedings of the European Conference on Computer Vision*, 2018, pp. 624–639.
- [54] J.-B. Grill, F. Strub, F. Altché, C. Tallec, P. Richemond, E. Buchatskaya, C. Doersch, B. Avila Pires, Z. Guo, M. Gheshlaghi Azar *et al.*, “Bootstrap your own latent—a new approach to self-supervised learning,” in *Proceedings of the Advances in Neural Information Processing Systems*, vol. 33, 2020, pp. 21 271–21 284.
- [55] K. He, H. Fan, Y. Wu, S. Xie, and R. Girshick, “Momentum contrast for unsupervised visual representation learning,” in *Proceedings of the IEEE/CVF conference on computer vision and pattern recognition*, 2020, pp. 9729–9738.
- [56] X. Chen and K. He, “Exploring simple siamese representation learning,” in *Proceedings of the IEEE/CVF Conference on Computer Vision and Pattern Recognition*, 2021, pp. 15 750–15 758.
- [57] W. Zhao, C. Li, W. Zhang, L. Yang, P. Zhuang, L. Li, K. Fan, and H. Yang, “Embedding global contrastive and local location in self-supervised learning,” *IEEE Transactions on Circuits and Systems for Video Technology*, vol. 33, no. 5, pp. 2275–2289, 2022.
- [58] Z. Chen, W. Wang, Z. Zhao, F. Su, A. Men, and Y. Dong, “Instance paradigm contrastive learning for domain generalization,” *IEEE Transactions on Circuits and Systems for Video Technology*, pp. 1–1, 2023.
- [59] D. Kim, Y. Yoo, S. Park, J. Kim, and J. Lee, “Selfreg: Self-supervised contrastive regularization for domain generalization,” in *Proceedings of the IEEE/CVF International Conference on Computer Vision*, 2021, pp. 9619–9628.
- [60] D. Du, J. Chen, Y. Li, K. Ma, G. Wu, Y. Zheng, and L. Wang, “Cross-domain gated learning for domain generalization,” *International Journal of Computer Vision*, vol. 130, no. 11, pp. 2842–2857, 2022.
- [61] J. Guo, L. Qi, and Y. Shi, “Domaindrop: Suppressing domain-sensitive channels for domain generalization,” in *Proceedings of the IEEE/CVF International Conference on Computer Vision*, 2023, pp. 19 114–19 124.
- [62] S. Shankar, V. Piratla, S. Chakrabarti, S. Chaudhuri, P. Jyothis, and S. Sarawagi, “Generalizing across domains via cross-gradient training,” in *International Conference on Learning Representations*, 2018.
- [63] Q. Xu, R. Zhang, Y. Zhang, Y. Wang, and Q. Tian, “A fourier-based framework for domain generalization,” in *Proceedings of the IEEE/CVF Conference on Computer Vision and Pattern Recognition*, 2021, pp. 14 383–14 392.
- [64] J. Li, Y. Li, H. Wang, C. Liu, and J. Tan, “Exploring explicitly disentangled features for domain generalization,” *IEEE Transactions on Circuits and Systems for Video Technology*, vol. 33, no. 11, pp. 6360–6373, 2023.
- [65] K. Zhou, Y. Yang, T. Hospedales, and T. Xiang, “Learning to generate novel domains for domain generalization,” in *Proceedings of the European conference on computer vision*, 2020, pp. 561–578.
- [66] Zhou, Kaiyang and Yang, Yongxin and Hospedales, Timothy and Xiang, Tao, “Deep domain-adversarial image generation for domain generalisation,” in *Proceedings of the AAAI conference on artificial intelligence*, 2020, pp. 13 025–13 032.
- [67] M. M. Rahman, C. Fookes, M. Baktashmotlagh, and S. Sridharan, “Multi-component image translation for deep domain generalization,” in *Proceedings of the IEEE Winter Conference on Applications of Computer Vision*, 2019, pp. 579–588.
- [68] A. Anoshch, E. Agustsson, R. Timofte, and L. Van Gool, “Combogan: Unrestrained scalability for image domain translation,” in *Proceedings of the IEEE/CVF conference on computer vision and pattern recognition workshops*, 2018, pp. 783–790.
- [69] J. Cha, S. Chun, K. Lee, H.-C. Cho, S. Park, Y. Lee, and S. Park, “Swad: Domain generalization by seeking flat minima,” in *Proceedings of the Advances in Neural Information Processing Systems*, 2021, pp. 22 405–22 418.
- [70] X. Chu, Y. Jin, W. Zhu, Y. Wang, X. Wang, S. Zhang, and H. Mei, “DNA: Domain Generalization with Diversified Neural Averaging,” in *International Conference on Machine Learning*, 2022, pp. 4010–4034.
- [71] A. Vaswani, N. Shazeer, N. Parmar, J. Uszkoreit, L. Jones, A. N. Gomez, Ł. Kaiser, and I. Polosukhin, “Attention is all you need,” in *Proceedings*

of the *Advances in Neural Information Processing Systems*, 2017, pp. 5998–6008.

- [72] D. Li, Y. Yang, Y.-Z. Song, and T. M. Hospedales, “Deeper, broader and artier domain generalization,” in *Proceedings of the IEEE/CVF International Conference on Computer Vision*, 2017, pp. 5543–5551.
- [73] M. Arjovsky, L. Bottou, I. Gulrajani, and D. Lopez-Paz, “Invariant risk minimization,” *arXiv preprint arXiv:1907.02893*, 2019.
- [74] S. Sagawa, P. W. Koh, T. B. Hashimoto, and P. Liang, “Distributionally robust neural networks,” in *International Conference on Learning Representations*, 2019.
- [75] S. Yan, H. Song, N. Li, L. Zou, and L. Ren, “Improve unsupervised domain adaptation with mixup training,” *arXiv preprint arXiv:2001.00677*, 2020.
- [76] D. Krueger, E. Caballero, J.-H. Jacobsen, A. Zhang, J. Binas, D. Zhang, R. Le Priol, and A. Courville, “Out-of-distribution generalization via risk extrapolation (rex),” in *Proceedings of the International Conference on Machine Learning*, 2021, pp. 5815–5826.
- [77] Z. Huang, H. Wang, E. P. King, and D. Huang, “Self-challenging improves cross-domain generalization,” in *Proceedings of the European conference on computer vision*, 2020, pp. 124–140.
- [78] G. Blanchard, A. A. Deshmukh, Ü. Dogan, G. Lee, and C. Scott, “Domain generalization by marginal transfer learning,” *The Journal of Machine Learning Research*, vol. 22, no. 2, pp. 46–100, 2021.
- [79] H. Nam, H. Lee, J. Park, W. Yoon, and D. Yoo, “Reducing domain gap by reducing style bias,” in *Proceedings of the IEEE/CVF Conference on Computer Vision and Pattern Recognition*, 2021, pp. 8690–8699.
- [80] M. Zhang, H. Marklund, N. Dhawan, A. Gupta, S. Levine, and C. Finn, “Adaptive risk minimization: Learning to adapt to domain shift,” in *Proceedings of the Advances in Neural Information Processing Systems*, 2021, pp. 23 664–23 678.
- [81] Y. Zhang, X. Wang, K. Jin, K. Yuan, Z. Zhang, L. Wang, R. Jin, and T. Tan, “Adanpc: Exploring non-parametric classifier for test-time adaptation,” in *Proceedings of the International Conference on Machine Learning*, 2023, pp. 41 647–41 676.
- [82] I. Gulrajani and D. Lopez-Paz, “In search of lost domain generalization,” in *International Conference on Learning Representations*, 2020.
- [83] C. Fang, Y. Xu, and D. N. Rockmore, “Unbiased metric learning: On the utilization of multiple datasets and web images for softening bias,” in *Proceedings of the IEEE/CVF International Conference on Computer Vision*, 2013, pp. 1657–1664.
- [84] L. Fei-Fei, R. Fergus, and P. Perona, “Learning generative visual models from few training examples: An incremental bayesian approach tested on 101 object categories,” in *Proceedings of the IEEE/CVF conference on computer vision and pattern recognition workshop*, 2004, pp. 178–178.
- [85] B. C. Russell, A. Torralba, K. P. Murphy, and W. T. Freeman, “Labelme: a database and web-based tool for image annotation,” *International journal of computer vision*, vol. 77, pp. 157–173, 2008.
- [86] M. J. Choi, J. J. Lim, A. Torralba, and A. S. Willsky, “Exploiting hierarchical context on a large database of object categories,” in *IEEE computer society conference on computer vision and pattern recognition*, 2010, pp. 129–136.
- [87] M. Everingham, L. Van Gool, C. K. Williams, J. Winn, and A. Zisserman, “The pascal visual object classes (voc) challenge,” *International journal of computer vision*, vol. 88, pp. 303–338, 2010.
- [88] H. Venkateswara, J. Eusebio, S. Chakraborty, and S. Panchanathan, “Deep hashing network for unsupervised domain adaptation,” in *Proceedings of the IEEE/CVF Conference on Computer Vision and Pattern Recognition*, 2017, pp. 5385–5394.
- [89] X. Peng, Q. Bai, X. Xia, Z. Huang, K. Saenko, and B. Wang, “Moment matching for multi-source domain adaptation,” in *Proceedings of the IEEE/CVF international conference on computer vision*, 2019, pp. 1406–1415.
- [90] J. Deng, W. Dong, R. Socher, L.-J. Li, K. Li, and L. Fei-Fei, “Imagenet: A large-scale hierarchical image database,” in *Proceedings of the IEEE/CVF Conference on Computer Vision and Pattern Recognition*, 2009, pp. 248–255.
- [91] L. Van der Maaten and G. Hinton, “Visualizing data using t-sne,” *Journal of machine learning research*, vol. 9, no. 11, pp. 2579–2605, 2008.
- [92] N. Srivastava, G. Hinton, A. Krizhevsky, I. Sutskever, and R. Salakhutdinov, “Dropout: a simple way to prevent neural networks from overfitting,” *The journal of machine learning research*, vol. 15, no. 1, pp. 1929–1958, 2014.
- [93] S. Ben-David, J. Blitzer, K. Crammer, A. Kulesza, F. Pereira, and J. W. Vaughan, “A theory of learning from different domains,” *Machine learning*, vol. 79, pp. 151–175, 2010.



Shaocong Long is currently pursuing his Ph.D. degree in the Department of Computer Science and Engineering, Shanghai Jiao Tong University. Before that, he received a B.E. degree in Nankai University in 2019. His current research interests focus on domain generalization, causal inference.



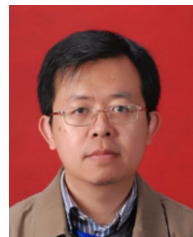
Qianyu Zhou is currently pursuing his Ph.D. degree in the Department of Computer Science and Engineering, Shanghai Jiao Tong University. Before that, he received a B.Sc. degree in Jilin University in 2019. His current research interests focus on computer vision, scene understanding, transfer learning. He serves regularly as a reviewer for IEEE TPAMI, IJCV, IEEE TIP, IEEE TCSVT, IEEE TMM, CVPR, ICCV, ECCV, AAAI, etc.



Chenhao Ying received the B.E. degree in the Department of Communication Engineering, Xidian University, China, in 2016, and the Ph.D. degree in the Department of Computer Science and Engineering, Shanghai Jiao Tong University, China, in 2022. He is currently a research assistant professor in the Department of Computer Science and Engineering, Shanghai Jiao Tong University. His current research interests include mobile crowd sensing, blockchain and federated learning.



Lizhuang Ma received his B.S. and Ph.D. degrees from the Zhejiang University, China in 1985 and 1991, respectively. He is now a Distinguished Professor, Ph.D. Tutor, and the Head of the Digital Media and Computer Vision Laboratory at the Department of Computer Science and Engineering, Shanghai Jiao Tong University, China. He was a Visiting Professor at the Frounhofer IGD, Darmstadt, Germany in 1998, and was a Visiting Professor at the Center for Advanced Media Technology, Nanyang Technological University, Singapore from 1999 to 2000. He published more than 400 academic research papers in both domestic and international journals. His research interests include computer-aided geometric design, computer graphics, computer vision, etc.



Yuan Luo received the B.S. degree in applied mathematics and the M.S. and Ph.D. degrees in probability statistics from Nankai University, Tianjin, China, in 1993, 1996, and 1999, respectively. From July 1999 to April 2001, he held a post-doctoral position with the Institute of Systems Science, Chinese Academy of Sciences, Beijing, China. From May 2001 to April 2003, he held another post-doctoral position with the Institute for Experimental Mathematics, University of Duisburg-Essen, Essen, Germany. Since June 2003, he has been with the Department of Computer Science and Engineering, Shanghai Jiao Tong University, Shanghai, China. Since 2006, he has been a Full Professor and the Vice Dean of the department (from 2016 to 2018 and since 2021). His current research interests include coding theory, information theory, and big data analysis.

APPENDIX

A. Proof for Proposition 1

Proof A.1: For the fixed semantics experts $\{E_i\}_{i=1}^M$ and feature extractor f , the minimax game in Eq. (10) in the main text reduces to the following maximizing problem:

$$\begin{aligned}
D^* &= \{D_1^*(\Phi', S'), D_2^*(\Phi', S'), \dots, D_M^*(\Phi', S')\} \\
&= \arg \max_D \sum_{i=1}^M \sum_{x,y} P_i^S(x, y) \log D_i(\Phi', S'), \\
&= \arg \max_D \sum_{i=1}^M \sum_{\Phi', S'} P_i^S(\Phi', S') \log D_i(\Phi', S'), \quad (14) \\
&\text{s.t.} \quad \sum_{i=1}^M D_i(\Phi', S') = 1.
\end{aligned}$$

We address this problem by maximizing the function point-wisely and then employing the Lagrangian multiplier:

$$\begin{aligned}
D^* &= \{D_1^*(\Phi', S'), D_2^*(\Phi', S'), \dots, D_M^*(\Phi', S')\} \\
&= \arg \max_D \left(\sum_{i=1}^M P_i^S(\Phi', S') \log D_i(\Phi', S') \right. \\
&\quad \left. + \lambda \left(\sum_{i=1}^M D_i(\Phi', S') - 1 \right) \right). \quad (15)
\end{aligned}$$

Setting the derivative of Eq. (15) w.r.t. $D_i(\Phi', S')$ to zero and combining the constraint $\sum_{i=1}^M D_i(\Phi', S') = 1$, we can obtain the following conclusion:

$$\lambda = - \sum_{i=1}^M P_i^S(\Phi', S'), D_i^*(\Phi', S') = \frac{P_i^S(\Phi', S')}{\sum_{j=1}^M P_j^S(\Phi', S')}. \quad (16)$$

B. Proof for Theory 1

Proof A.2: If D^* is the optimum for the inner maximization of Eq. (10) in the main text, then the minimax game of Eq. (10) in the main text reduces to the following minimizing problem:

$$\begin{aligned}
\min_f -H(D(\Phi, S)) &= \min_f \sum_{i=1}^M \sum_{x,y} P_i^S(x, y) \log \frac{P_i^S(\Phi, S)}{\sum_{j=1}^M P_j^S(\Phi, S)} \\
&= \min_f \sum_{i=1}^M \sum_{\Phi, S} P_i^S(\Phi, S) \log \frac{P_i^S(\Phi, S)}{\sum_{j=1}^M P_j^S(\Phi, S)} \\
&\quad + M \log M - M \log M \\
&= \min_f \sum_{i=1}^M \sum_{\Phi, S} P_i^S(\Phi, S) \log \frac{P_i^S(\Phi, S)}{\frac{1}{M} \sum_{j=1}^M P_j^S(\Phi, S)} + C \\
&= \min_f \sum_{i=1}^M KL(P_i^S(\Phi, S) || \frac{1}{M} \sum_{j=1}^M P_j^S(\Phi, S)) + C \\
&= \min_f M \cdot JSD(P_1^S(\Phi, S), P_2^S(\Phi, S), \dots, P_M^S(\Phi, S)) + C, \quad (17)
\end{aligned}$$

where $C = -M \log M$ is a constant. Thus the minimax game in Eq. (10) in the main text is equivalent to matching the semantic-based distributions in Eq. (6) in the main text, and the global optimum of Eq. (10) in the main text can be attained if and only if $P_1^S(\Phi, S) = P_2^S(\Phi, S) = \dots = P_M^S(\Phi, S)$.